LEGIBILITY NOTICE

A major purpose of the Technical Information Center is to provide the broadest dissemination possible of information contained in DOE's Research and Development Reports to business, industry, the academic community, and federal, state and local governments.

Although a small portion of this report is not reproducible, it is being made available to expedite the availability of information on the research discussed herein.

LA-UR--89-1161

DE89 011196

MAY [illegible]

[illegible]

[illegible]

[illegible]

[illegible]

Los Alamos National Laboratory
Los Alamos, New Mexico 87545

APPLICATIONS OF INFRARED LASER SPECTROSCOPY TO LASER CHEMISTRY AND LASER DEVELOPMENT

Robin S. McDowell

University of California, Los Alamos National Laboratory,
Los Alamos, New Mexico 87545, U.S.A.

ABSTRACT

The impact on infrared molecular spectroscopy of high resolution tunable laser sources and laser-controlled Fourier-transform spectrometers is discussed, with special reference to rovibrational spectra of spherical-top molecules such as CH_4, OsO_4, SiF_4, SF_6, and UF_6. The role of tunable laser spectroscopy in analyzing the CF_4 laser, resulting in the precise prediction of lasing frequencies between 615 and 655 cm^{-1}, is described. Studies of overtone and combination bands of SF_6 enable the vibrational anharmonicity to be determined, resulting in a more detailed description of the pump transitions involved in laser photochemistry, and of higher vibrational levels and pathways to excitation and dissociation. This permits more accurate calculations of vibrational state densities for spherical-top molecules. Implications for the photochemistry of species such as SiF_4, SF_6, UF_6, and $Ni(CO)_4$ are discussed.

1. INTRODUCTION

During the last quarter century the development of lasers has had a great impact on the field of molecular spectroscopy. Shortly after the invention of lasers in 1960, these intense, monochromatic light sources were applied to Raman spectroscopy. Cumbersome Toronto mercury arcs were quickly replaced by lasers, and the field underwent a renaissance that continues today.

Applications of lasers to infrared spectroscopy had to await the development of tunable sources. These began to appear about 1970, and their development over the next decade resulted in the emergence of several classes of tunable lasers whose usefulness in the infrared is now well established. A significant fraction of all work in infrared spectroscopy now involves the direct use of tunable monochromatic sources, and if one considers in addition spectra recorded with interferometers, whose optical path differences are monitored with fixed frequency lasers, the impact of lasers on the field is overwhelming. A beneficial synergism has resulted, in which studies of atomic and molecular energy levels have in turn led to the development of new laser systems.

The high energy density available from lasers has also revolutionized the field of photochemistry, as intense sources have been used to pump specific molecular transitions up to highly excited states, and on to dissociation. This has given new significance to

higher vibrational states, vibrational ladders, and details of anharmonicity, and these studies have been possible only because of the increase in resolution that lasers have brought to the infrared region of the spectrum.

A full treatment of the related fields of molecular spectroscopy, tunable lasers, and laser photochemistry would by now require several volumes, and certainly won't be attempted here. We will consider instead some of the research in these areas conducted at Los Alamos over the last 15 years, concentrating on those aspects that best illustrate the interdependence of spectroscopy, lasers, and photochemistry. It happens that much of the work described here involves spherical-top molecules (i.e., those with three equal moments of inertia). We will emphasize spectra of molecules of this class having tetrahedral (XY_4) or octahedral (XY_6) symmetry, but the principles involved are more broadly applicable, and references will be provided to literature dealing with other species.

2. HIGH-RESOLUTION INFRARED TECHNIQUES

Until about a generation ago, all infrared spectroscopy was carried out with dispersive spectrometers that used prisms or diffraction gratings as the dispersive elements. Prism instruments can achieve resolutions of no better than about 1 cm^{-1} near wavelengths of maximum dispersion, and usually significantly poorer than this. Grating resolution varies less with wavenumber, and can be of the order of several tenths of a cm^{-1} for commercial spectrometers, though some specially built research instruments can with difficulty resolve a few hundredths of a cm^{-1}.

These values should be compared with typical linewidths of infrared transitions in gaseous molecules. At low pressures, for which collision broadening is negligible, the full Doppler width at half maximum absorption (fwhm) is given by $\Delta\nu = 7.16\times10^{-7}\nu(T/M)^{1/2}$, where the transition frequency ν is in cm^{-1}, the molecular weight M in amu, and the temperature T in K. So lines in the rovibrational spectrum of SF_6 at 10 μm and room temperature will have fwhm of ca. 0.001 cm^{-1}, an order of magnitude less than the resolution of the best grating research spectrometers. We can see why improved resolution has been a constant concern of infrared spectroscopists.

2.1 Fourier-Transform Spectrometers

A century ago A. A. Michelson invented the Michelson interferometer, in which light strikes a partially reflecting beamsplitter plate at an angle of 45° and is divided into two beams which are returned by mirrors and recombined at the beamsplitter. The intensity of the recombined and interfering beams, recorded as a function of the optical path difference as one mirror is moved, yields an *interferogram*. Michelson recognized, as did Lord Rayleigh, that from the Fourier transform of such an interferogram one could in principle recover the desired spectrum, i.e., the source intensity as a function of wavelength. However, computational difficulties in carrying out the

transform rendered this technique impracticable except for certain specialized studies of the fine structure of atomic lines.

In the 1950's two discoveries renewed interest in potential applications of Fourier-transform spectrometers (FTS's). Fellgett emphasized the *multiplex advantage* of interferometers over spectrometers, in that the former record information from all spectral elements simultaneously instead of sequentially. At the same time, as shown by Jacquinot, interferometers have a *throughput advantage*, passing much greater light flux for a given resolving power. The computational problems were reduced by the discovery of the fast Fourier transform by Cooley and Tukey in 1965; and with the ready availability of inexpensive computers, FTS became the accepted technique for high-performance infrared spectroscopy. Several texts treat modern Fourier-transform spectroscopy in detail.[1,2]

Most infrared spectrometers marketed today are actually Michelson interferometers with an associated computer to perform the Fourier transform and handle and display the spectral output. These have been designed to meet a broad range of requirements, from routine analyses for which low resolution is adequate, to research instruments, of which the most recently announced claims a resolution of 0.002 cm^{-1}.

2.2 The Los Alamos Fourier-Transform Spectrometer

In addition to the commercial instruments mentioned above, special purpose high-performance Fourier-transform spectrometers have been designed and built in several laboratories. Examples are James Brault's FTS at Kitt Peak National Observatory, Arizona[3]; Guy Guelachvili's interferometers at Université de Paris-Sud[4]; and Jyrki Kauppinen's mid- and far-infrared spectrometers at the University of Oulu, Finland.[5] We will describe here another such instrument, recently built at Los Alamos National Laboratory by Byron Palmer, with design consultation by Jim Brault.[6,7]

The Los Alamos instrument was designed to provide the best available spectral resolution, signal to noise ratio, and photometric accuracy, from 200 nm in the ultraviolet to 20 μm and beyond in the mid infrared. It consists of a two-arm folded-path Michelson interferometer with two moving cat's-eye reflectors; the optical system is shown in Fig. 1. This arrangement avoids the necessity for frequent dynamic alignment, as is required with other mirror systems. Each mirror travels about 1 m for a total optical path difference of 2 m, resulting in a resolution of 0.0025 cm^{-1} (i.e., resolving powers of 10^5 to 10^7). A double pass system will improve the resolution to 0.0013 cm^{-1} when required, though it has not yet been operated in this mode.

The mirror carriages are moved on horizontal oil bearings by linear motors at constant velocity. A closed servo system based on a stabilized Zeeman split He-Ne laser controls piezoelectric elements on the cat's eye secondaries, providing fine motion control with frequency response to a kHz. The mirror positions are monitored to within 1 Å, resulting in a wavenumber accuracy of 10^{-5} cm^{-1}. The pairs of beamsplitters are mounted on a rotating turret, allowing different

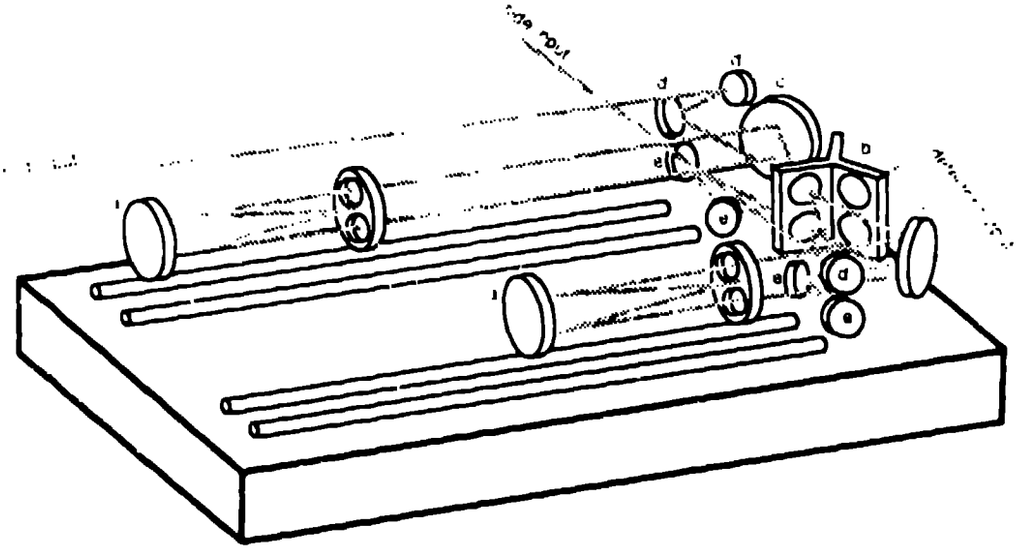

Fig. 1. Optical system of the Los Alamos Fourier-transform spectrometer, showing the cat's-eye reflectors (a), beam splitter turret (b), folding mirrors (c), collimating optics (d), and detector optics (e). The mirrors (a) and (c) are 8 in (20 cm) in diameter. Illustration from Palmer.[7]

spectral regions to be conveniently accessed. The entire assembly is contained in a 14 × 7 ft cylindrical vacuum tank, so that absorption due to atmospheric gases is avoided.

The digitizing electronics have a 22-bit dynamic range (4×10^6), yielding an intensity precision of the order of 0.1%. The instrument is controlled by Macintosh computers, which perform the fast Fourier transforms of the interferograms, display the spectra, generate line files, fit line profiles, etc. The maximum number of points is 4 million, limited by disk storage, and a transform of this size requires 2.3 hr to compute.

The Los Alamos FTS has been operational in the ultraviolet through near-infrared regions for two years, and full mid-infrared operation commenced early in 1989. The instrument has satisfactorily met its design specifications throughout its wavenumber range.

Figure 2 illustrates a portion of the methane fundamental originating at 3019 cm^{-1}, recorded to test the resolution of the instrument, here nominally 0.0054 cm^{-1} as calculated from the maximum optical path difference. The only line-broadening mechanism effective at this low pressure is that due to the Doppler effect, calculated from the expression given above to be 0.0097 cm^{-1}. Taking the root sum square of the instrumental and Doppler widths yields an expected fwhm of 0.0107 cm^{-1}, which compares satisfactorily with measured linewidths of 0.011 ± 0.001 cm^{-1} in Fig. 2. The tensor splitting of this P(6) transition into six component lines is due to centrifugal effects, and is characteristic of spherical top molecules. We will encounter other

examples of this in the following sections.

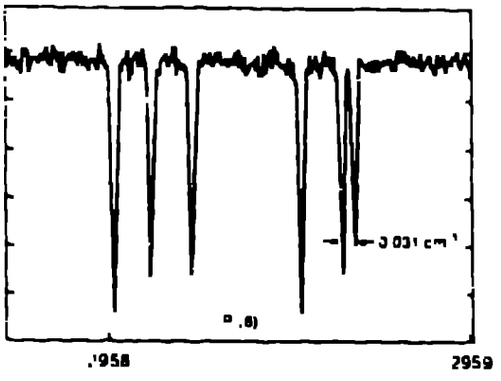

Fig. 2. The P(6) manifold of the ν_3 stretching fundamental of CH_4, recorded with the Los Alamos Fourier-transform spectrometer. Sample pressure 1 Torr. The scale on the bottom is in cm^{-1}.

2.3 Tunable Laser Sources

While the best interferometers can achieve resolution of the order of 10^{-1} cm^{-1}, there are many situations in which still higher infrared resolution is useful: for example, in precise studies of line contours and intensities, and for spectroscopy of heavy molecules in the vapor phase. Since FTS resolution is directly proportional to the maximum optical path difference, a point is reached at which any further improvement entails formidable optical and mechanical design difficulties with the moving mirror(s). Spectroscopists then turn to tunable lasers, which have been developed into very useful spectroscopic tools over the last 20 years. The technique is conceptually very simple: radiation from an essentially monochromatic source is passed through the sample, without the need for any spectrometer or interferometer, and the spectrum is obtained by tuning the output frequency of the source. (This apparent simplification is somewhat counteracted by the fact that tunable lasers tend to be complex and fractious devices with their own difficulties that must be dealt with.)

Tunable laser spectroscopy has generated an immense literature. Here we will only briefly outline the devices available, and refer the reader to reviews covering tunable sources themselves and the types of spectroscopic investigations that are being carried out with them.[4-7]

Tunable lasers that have been used in spectroscopy are listed in Table 1.[7] Several other devices or techniques have been investigated but never fully developed for high-resolution spectroscopy: polariton lasers, optical parametric mixing, four-wave parametric mixing, vibronic transition lasers, etc.; for details see the review papers cited.[4-7] The coverage given in Table 1 is the wavelength region for which laser action has been demonstrated, which doesn't necessarily imply that a useful spectroscopic technique has been developed. Figure 3 shows those regions in which the results of high resolution spectroscopic studies have actually been reported, and is a more realistic guide to the spectral coverage available. Also shown in Fig. 3 is a rough indication of the percentage of papers in which the various techniques have been used.

The important conclusion to be drawn from Table 1 and Fig. 3 is that tunable laser sources are available to cover much of the mid-infrared region with resolutions of 10^{-4} to 10^{-5} cm^{-1}, orders of magni-

Table 1 Spectroscopically Useful Tunable Laser Sources

Device	Coverage (μm)	Maximum resolution (cm^{-1})	Typical CW power (W)
Semiconductor diode lasers	0.4-34	2×10^{-6}	10^{-3}
Gas lasers:			
Waveguide CO_2 lasers	9-11[a]	3×10^{-7}	1
Zeeman-tuned gas lasers	0.6-9[a]	1×10^{-3}	10^{-1}
Spin-flip Raman lasers	5.0-6.5	1×10^{-6}	0.1
Nonlinear optical mixing techniques:			
Difference frequency generation	0.7-24.3	1×10^{-4}	10^{-6}
Tunable sideband generation	3.4	2×10^{-10}	?
	9.1-11.3	1×10^{-5}	10^{-3}
Color-center lasers	0.35-4.0	9×10^{-6}	10^{-2}

[a] Tunable only near discrete lines in this region.

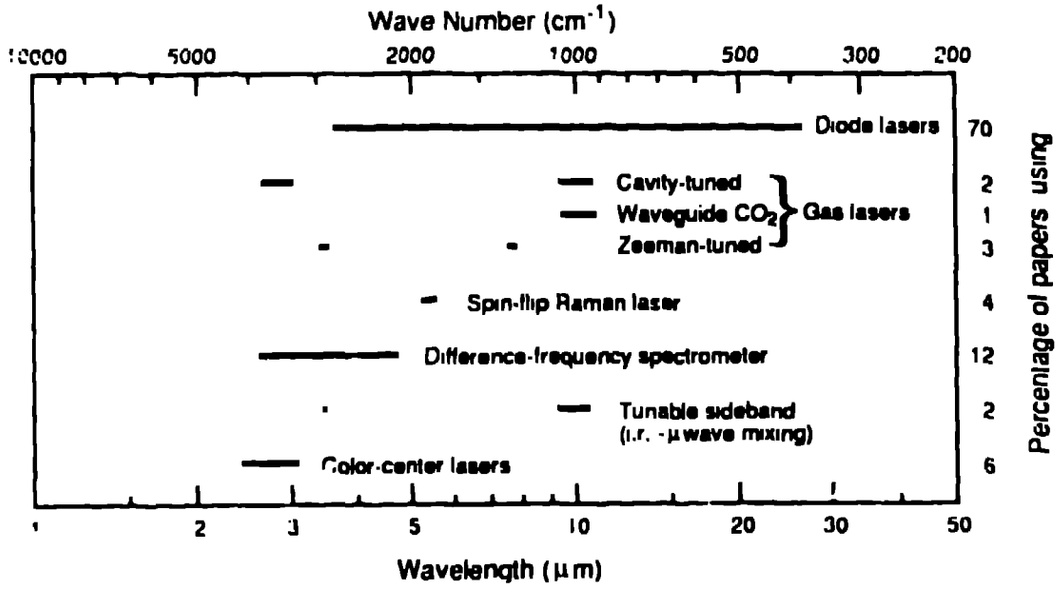

Fig. 1. Regions of demonstrated spectroscopic coverage of various tunable high-resolution infrared laser sources.[3]

wide less than the Doppler widths of most molecules. Many of these devices are readily tunable over only very limited wavelength ranges, and consequently FTS instruments are often preferable; but when resolution is at a premium the tunable lasers are invaluable. In the following sections we will discuss different research areas in which other lasers or interferometers were the technique of choice.

3 IMPACT OF HIGH-RESOLUTION INFRARED SPECTROSCOPY

3.1 Sulfur Hexafluoride

SF_6 has an intense stretching fundamental at 948 cm^{-1}, which overlaps many of the emission lines of the CO_2 10.4-μm laser band. Several features of this fundamental contributed to making it one of the most thoroughly-studied molecular transitions, soon after the development of tunable diode lasers: the relatively large moment of inertia of SF_6 causes very closely-spaced rotational structure that can not be resolved by traditional spectroscopy; another consequence of this is that total angular momentum states up to J=100 and above are readily accessible at room temperature, and such states can not be observed in light molecules such as CH_4; many interactions between SF_6 and CO_2 laser radiation had been investigated, such as saturation, self-induced transparency, optical nutation, photon echoes, Q-switching, double resonance, laser-induced fluorescence and dissociation, and isotope separation,[10] and the identity of the precise SF_6 transitions pumped in these experiments was in question; and, finally, SF_6 was a useful prototype molecule for species such as UF_6, which was being considered for laser isotope separation, and which has an even more complex spectrum than does SF_6.

Figure 4 illustrates the fundamental in question at resolutions of ca. 10, 0.07, 0.001, and 10^{-6} cm^{-1}. It consists of poorly-resolved P, Q, and R branches, in each of which the J manifolds are split into their tensor components as is P(6) of methane in Fig. 2. But much higher J manifolds are populated in SF_6, and the spacing between them is such that they overlap in the P and R branches beginning at J ≈ 22, so SF_6 exhibits a much more complex rovibrational spectrum than does a hydride molecule such as CH_4, as panel (c) of Fig. 4 indicates. Even an apparently single transition at Doppler-limited resolution shows further structure when sub-Doppler saturation spectroscopy is employed, panel (d).

In the late 1970's tunable diode lasers were used to resolve the structure across much of the SF_6 band at the Doppler limit, and many thousands of lines were assigned.[11-13] In Q-branch regions such as that shown in panel (c) of Fig. 4, where line overlap is extreme, special techniques were developed for making assignments, including band synthesis by computer.[14] As a result of this work, the spectroscopic constants of this band were accurately determined.[15] At the same time, Fourier-transform and diode-laser spectra of the bending fundamental ν_4 at 615 cm^{-1} were being analyzed, including lines up to P(100).[16]

The most recent analysis of ν_3 was made by Bobin et al.,[17] who fit the spectroscopic constants to 136 transitions accurately measured by saturation spectroscopy with uncertainties of 5 kHz (2×10^{-7} cm^{-1}). They obtained 24 constants with unprecedented precision; for example, the ground state rotational constant B_0 = 0.09108520016(10) cm^{-1}, and the band origin is ν_3 = 948.1025234(6) cm^{-1}. These uncertainties compare with or surpass even those obtainable from microwave spectroscopy which of course can not be used for spherical top molecules, which

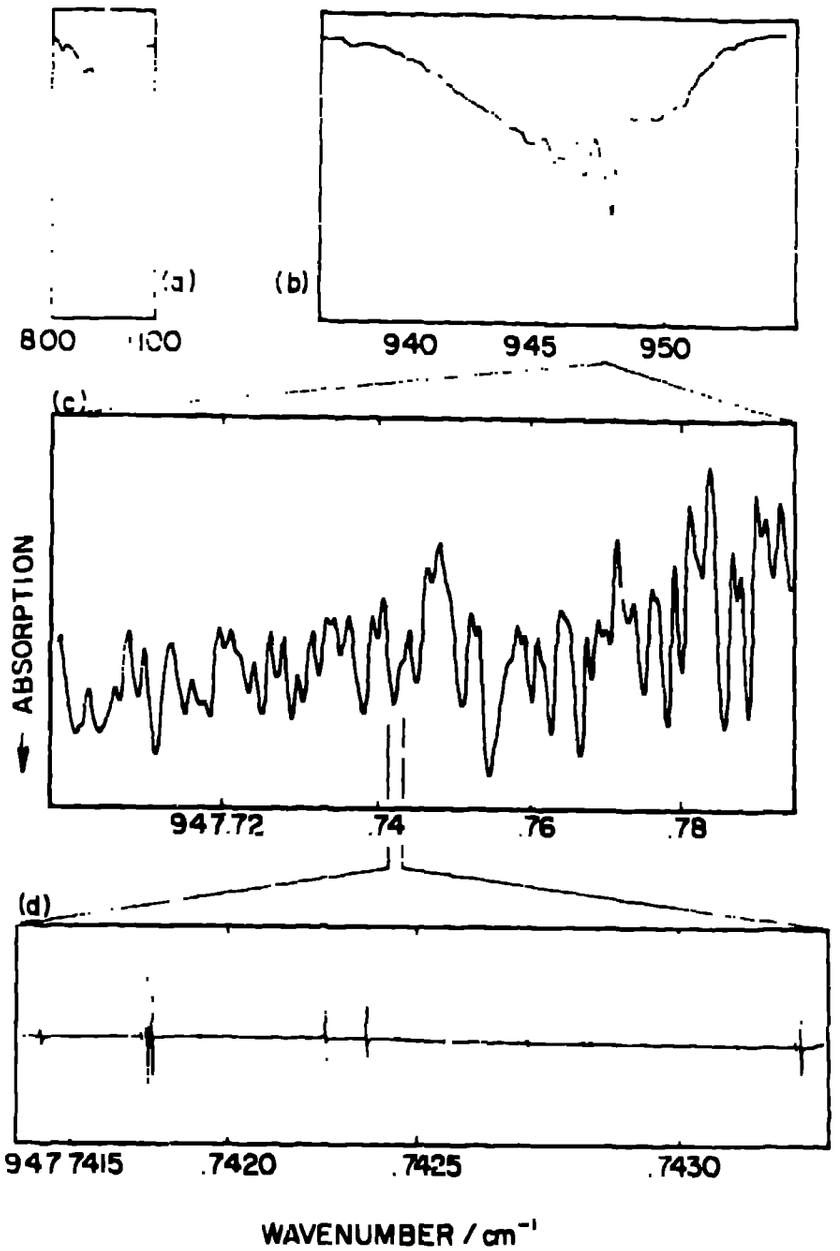

Fig. 4. The infrared-active stretching fundamental ν_3 of SF_6 as it appears with increasing resolving power. (a) Early prism spectrum (Eucken & Ahrens, 1934). (b) Spectrum at 0.07 cm^{-1} resolution (Brunet & Perez, 1969). (c) A portion of the Q branch recorded with a tunable semiconductor diode laser (Hinkley, 1970); laser linewidth $<10^{-5}$ cm^{-1}, but the effective resolution is the Doppler width of 0.001 cm^{-1}. (d) Sub-Doppler saturation spectrum recorded (in the derivative mode) inside the gain profile of the P(16) line of a CO_2 laser (Clairon & Henry, 1977); effective resolution $\sim 10^{-4}$ cm^{-1}. From Reference 8.

lack permanent dipole moments).

Considering the high-resolution spectroscopy of the higher vibrational levels of SF_6 that will be discussed in §5, together with other work such as stimulated Raman gain spectroscopy of the infrared-inactive fundamentals,[9] the spectroscopic properties of SF_6 are perhaps better known than those of any other molecule. This work has, in turn, greatly stimulated theoretical investigations into the analysis of rovibrational energy levels and transitions, and the development of model Hamiltonians that can adequately account for data of this precision.

3.2 Identification of Laser-Pumped Transitions

One of the reasons for detailed rovibrational studies in the infrared is the importance of knowing just what transitions are pumped by laser radiation in the types of experiments mentioned in the first paragraph of § 3.1. Since the 00^01-[$10^00,02^00$] CO_2 laser transitions (between 900 and 1100 cm^{-1} for $^{12}C^{16}O_2$) are the most useful source of intense monochromatic light in the mid-infrared, many molecules that absorb in the 9-11 μm region have been intensively studied.[10]

The initial work on SF_6[11-13] identified the specific transitions that are in resonance with the six CO_2 laser lines from P(12) [951.19 cm^{-1}, near R(66) of SF_6] to P(22) [942.38 cm^{-1}, near P(84) of SF_6]. For example, the triplet at 947.7417 cm^{-1} in panel (d) of Fig. 4 consists of the $F_1^{3-}E^0+F_2^0$ lines of Q(38), and the center of these is detuned from CO_2 P(16) by -7 MHz $\approx -2 \times 10^{-4}$ cm^{-1}.[12] These assignments immediately answered some questions about the nature of pulse breakup in self-induced transparency experiments. It was apparent that ideal pulse breakup requires only near-coincidence with a nonoverlapped P or R transition, not necessarily a nondegenerate one, as some had suspected.[13] Since then Bobin et al.[17] have assigned more SF_6 lines near the CO_2 frequencies, have also measured some near R(10) of the N_2O laser, and have predicted those near emission frequencies of the $^{12}C^{16}O^{18}O$, $^{12}C^{18}O_2$, $^{13}C^{16}O_2$, and $^{13}C^{18}O_2$ lasers.

The rovibrational spectra of several other molecules that absorb in the CO_2 laser region have been reported. The ν_2/ν_4 bending diad of $^{13}CD_4$ was recorded with a Fourier-transform instrument at a resolution of 0.04 cm^{-1} and analyzed.[19] This band is of interest in connection with infrared-radiofrequency double resonance experiments; state-to-state rotational relaxation[20]; and because several very close $^{13}CD_4/CO_2$ coincidences may be useful in the rapid, inexpensive detection and analysis of $^{13}CD_4$, a sensitive nonradioactive atmospheric tracer useful in monitoring air-mass movements.

Another well-studied molecule is OsO_4, whose ν_1 fundamental is at 961 cm^{-1}. From an analysis of Fourier-transform and tunable diode laser spectra of $^{187}OsO_4$, $^{189}OsO_4$, and $^{192}OsO_4$, transitions of all isotopic species that were expected to fall near CO_2 laser lines were calculated.[21] Recently a more detailed analysis was made using higher-resolution Fourier-transform data on natural OsO_4.[22] This molecule is of particular interest because unlike most other spherical

tops, its ligand atoms have zero nuclear spin, and consequently only rotational levels of A symmetry exist. For example, no transitions occur in OsO_4 corresponding to the F+E+F triplet at 947.7417 cm^{-1} in SF_6 [Fig. 4(d)]. This greatly simplifies the rovibrational spectrum compared with molecules such as CH_4 and SF_6. Figure 5 illustrates this at the beginning of the Q branch. Since there are no A levels for J = 1, 2, and 5, the Q branch starts with the transitions Q(3), Q(4), Q(6), ..., the usual Q(1) line very close to the band origin ν_3 = 960.805 cm^{-1} is missing. [Q(0) is, of course, not dipole-allowed in any case.] And, for example, Q(17) has two lines in OsO_4 ($A_1^2+A_2^2$), compared with 14 ($A_1+A_2+3E+5F_1+4F_2$) in other spherical tops.

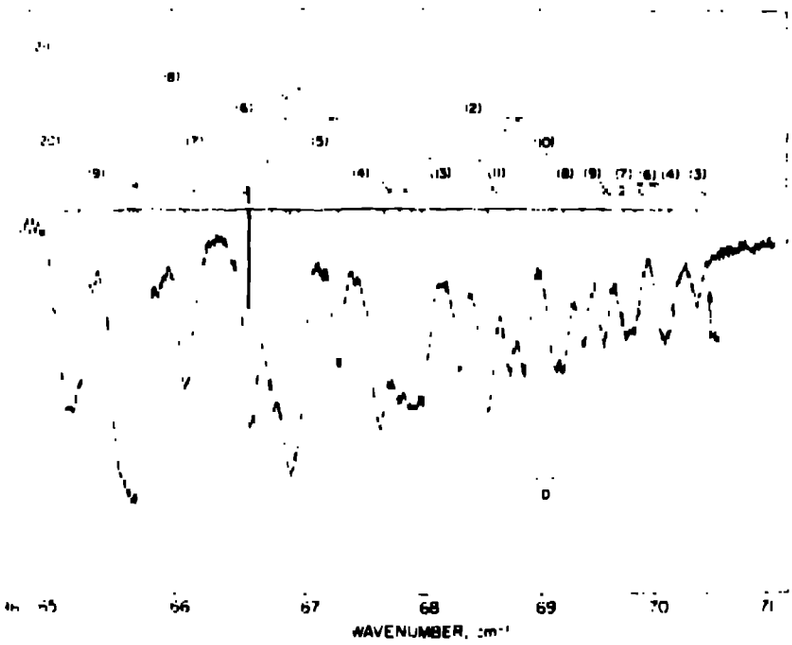

Fig. 5. Start of the Q branch of $^{192}OsO_4$, recorded with a tunable semiconductor diode at a gas temperature of 245 K. Lines are identified with the notation $(15)_{21}$ = Q(15) A_2^1, etc. The Doppler fwhm, 6.7×10^{-4} cm^{-1}, is indicated by D. From Reference 21.

The ν_3 fundamental of SiF_4 at 1031 cm^{-1} is another that has been studied specifically to identify CO_2 laser coincidences.[23,24] Both Doppler-limited diode spectra and sub-Doppler saturation spectra were obtained, and separate fits to the two sets of data yielded nearly identical spectroscopic constants. It was shown that the CO_2 P(36) laser line does not coincide with any ground-state transition of SiF_4, thus probably accounting for earlier unsuccessful attempts using this pump frequency to induce an isotopically-selective $SiF_4 + H_2$ reaction.

Finally, mention should be made of the ν_1 stretch of UF_6.[25] This occurs at 628 cm^{-1}, well outside the CO_2 region, but is of interest for its potential usefulness in the laser isotope separation of uranium. Experiments on UF_6 included exciting it with the CF_4 laser, and the exact transitions pumped were of course of great importance. The CF_4 laser itself will be discussed in the next section.

4. SPECTROSCOPY OF LINE-TUNABLE GAS LASERS: CF_4

A proper understanding of any optically-pumped molecular gas laser system requires a detailed analysis of the rovibrational energy levels involved in the pump and laser transitions. Much work on the spectroscopy of such molecules as HF, CO, CO_2, C_2H_4, CH_3OH, and C_2D_2 has been stimulated by interest in their lasing properties. A discussion of the analysis of one specific laser molecule, CF_4, will illustrate the close interaction between molecular spectroscopy and laser development.

When the combination band $\nu_2+\nu_4$ of CF_4 at 1066 cm^{-1} is pumped by the 9.4-μm CO_2 laser, stimulated emission on the $(\nu_2+\nu_4) \rightarrow \nu_2$ transition produces many discrete laser lines in the region 605 to 655 cm^{-1}. Analysis of this system started with a tunable diode laser study of the $\nu_2+\nu_4$ pump band, which allowed rough estimates of the lasing frequencies.[26] These frequencies were then measured with a 1-m grating monochromator to an accuracy of ± 0.2 cm^{-1}, yielding a preliminary determination of the spectroscopic constants of the infrared-inactive ν_2 fundamental.[27] Diode laser spectra of the ν_4 region[28] finally led to the identification of a series of $(\nu_2+\nu_4) \leftarrow \nu_2$ hot-band transitions, corresponding to many of the laser lines but now seen in absorption rather than emission.[29] From these data the spectroscopic constants were refined, and it was possible to predict, for any given CO_2 pump transition between 1050 and 1085 cm^{-1}, the resulting laser line or lines with an accuracy of 0.01 to 0.003 cm^{-1}.[29]

One of the strongest CF_4 laser lines is at 615 cm^{-1}, obtained by pumping with CO_2 R(12). Figure 6 shows the transitions involved: R(12) is nearly resonant with a strong line (actually a A+E+F cluster) of CF_4, detuned by only 19 MHz = 6×10^{-4} cm^{-1}, and identified as belonging to R'(29) of $\nu_2+\nu_4$. [Since the F_1 ("inactive") and F_2 (infrared-active) sublevels of $\nu_2+\nu_4$ are separated by only 0.58 cm^{-1}, they are strongly mixed, and the resulting band exhibits all nine possible subbranches of a spherical-top transition, instead of only R, Q, and P as for a fundamental.] This transition is shown on the right side of Fig. 6: the upper-state F_2 level of $J' = 30$ is populated, and stimulated emission occurs on the transition to $J = 31$ of ν_2, producing the laser line P'(31) at 615.03 cm^{-1}. If the CO_2 laser has a linewidth of a few hundred MHz, it is apparent from Fig. 6 that a R'(28) line of CF_4 will also be pumped; this results in a different, weaker, laser line, P'(30) at 615.70 cm^{-1}. In many cases two nearly coincident pump transitions will belong to different branches, and give rise to laser emission at widely separated frequencies. Some 40 observed laser transitions have thus been accounted for in detail, and it has become possible to search for pump lines of isotopic CO_2 lasers that will produce specific output frequencies in the 16 μm region.

5. HIGHER VIBRATIONAL LEVELS AND ANHARMONICITY

5.1 Overtones of Pump Transitions and Multiphoton Ladders

Most molecules have only a few strong absorptions which are to

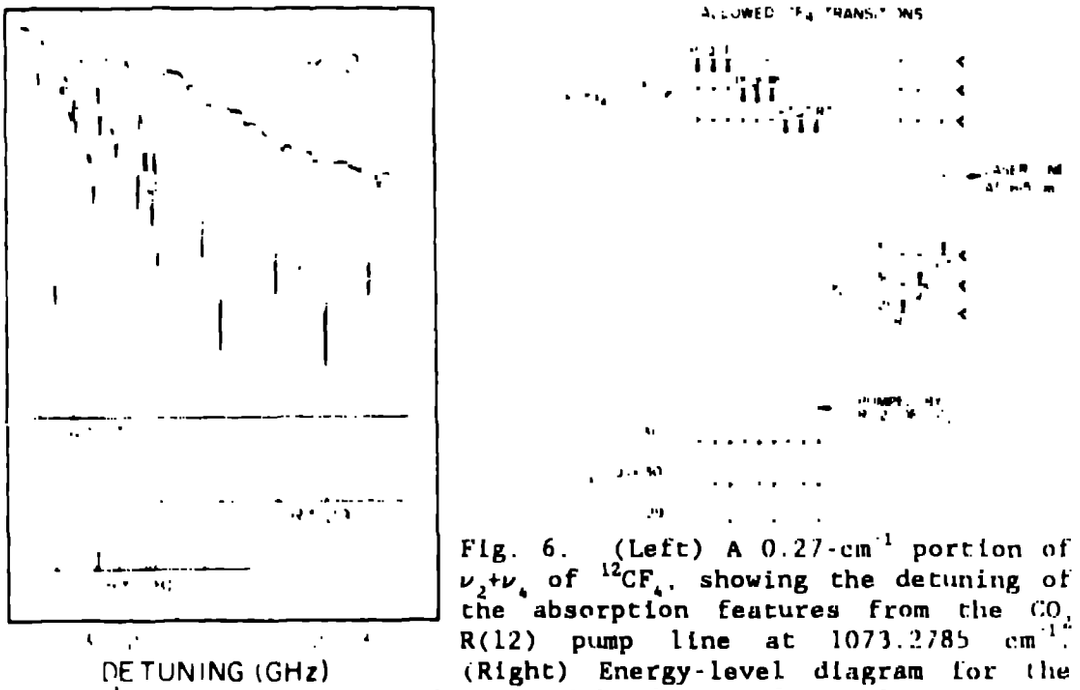

Fig. 6. (Left) A 0.27-cm^{-1} portion of $\nu_2+\nu_4$ of $^{12}CF_4$, showing the detuning of the absorption features from the CO_2 R(12) pump line at 1073.2785 cm^{-1}. (Right) Energy-level diagram for the 615-cm^{-1} line of the $^{13}F_4$ laser, with the total angular momentum quantum numbers in the vibrational ground state, $\nu_2+\nu_4$, and ν_3 denoted by J_3, J', and J, respectively. From Refs. 26, 27, 29.

the proper wavelength region to be considered as pump frequencies for photochemistry experiments. For tetrahedral (XY_4) and octahedral (XY_6) species these tend to be the infrared-active stretching fundamentals, which (by coincidence) are designated ν_3 in both cases. In particular, ν_3 of OsO_4 (961 cm^{-1}), SiF_4 (1031 cm^{-1}), and SF_6 (948 cm^{-1}) all fall in the region of CO_2 laser emission, and have been the objects of numerous pumping experiments. After one of these molecules absorbs a ν_3 photon, the next excitation is $2\nu_3 \leftarrow \nu_3$, and then $3\nu_3 \leftarrow 2\nu_3$, etc.; excitation takes place up the $n\nu_3$ ladder, with some leakage into adjoining vibrational states, until the *quasicontinuum* is reached, by which point numerous nearly-coincident vibrational states are accessible. The exact nature of the lower portions of this ladder will determine the physical and photochemical behavior of the molecules as they absorb the pump frequency.

In considering the structure of higher vibrational states in spherical-top molecules, three effects must be considered: (1) Vibrational anharmonicity, which displaces a overtone ($n\nu_3$) from its harmonic frequency: $(n\nu_3) = n\nu_3 + n(n-1)X_{33}$, where X_{33} is an anharmonicity constant (usually negative). (2) The splitting of higher states into rotands. For a vibrational fundamental of symmetry f_{3u} (such as ν_3 of SF_6), the first and second overtones $2\nu_3$ and $3\nu_3$ have the level structures $A_{1g}+E_g+F_{2g}$ and $A_{2u}+2F_{1u}+F_{2u}$, respectively, of which to a first approximation only the F_{1u} levels are infrared active. In the formalism of Hecht,[31] the displacements of these individual sublevels from

the manifold origin is determined by constants designated, for the ν_3 ladder, G_{33} and T_{33}. (3) The broadening of the vibrational levels by rotational structure. This broadening in the case of ν_3 of SF_6 is of the order of 15 cm^{-1} [Fig. 3(b)], but differs for other vibrational levels, especially those in which additional branch transitions are allowed: $\nu_2+\nu_4$ of CF_4 discussed in §4 is an example of this.

In principle, two vibrational manifolds in the $n\nu_3$ ladder of a spherical top -- say the ν_3 fundamental itself and one overtone -- yield the values of the effective harmonic frequency and of the principal anharmonicity constants X_{33}, G_{33}, and T_{33} that are needed to specify the ladder structure.[31] For tetrahedral species, this is relatively straightforward; but for octahedral molecules, $2\nu_3 \leftarrow 0$ is dipole forbidden, and these constants must be deduced either from the very weak second overtone ($3\nu_3 \leftarrow 0$) or from double-resonance spectroscopy of hot bands such as $2\nu_3 \leftarrow \nu_3$.

For SF_6, several studies of the $3\nu_3$ overtone (2828 cm^{-1}) were made using grating[32] and FTS[33] data, but the assignments and analysis remained in question until a Doppler-limited spectrum recorded with a difference-frequency spectrometer was analyzed by Pine and Robiette,[34] and later in more detail by Patterson et al.[35] Some of these constants were also derived from the $2\nu_3 \leftarrow \nu_3$ transition seen in a double-resonance pump-probe experiment.[36] Some absorptions seen in spectra of the ν_3 region obtained with high-intensity sources (ca. 1 MW/cm^2) could be assigned to two-photon resonances between the ground state and $2\nu_1$.[36,37] The $n\nu_3$ ladder of SF_6 is now perhaps as well understood as that of any molecule.[37]

A difference-frequency spectrometer has been used to record $3\nu_1$ of SiF_4 at 3069 cm^{-1}, and values of X_{11}, G_{11}, and T_{11} were obtained from the analysis.[38]

Recently, an attempt at a similar analysis, using tunable diode laser spectra, was made for $3\nu_1$ of UF_6 (1876 cm^{-1}).[11] The difficulties in this work were severe, for the low vapor pressure of UF_6 required pathlengths of up to 400 m, and even then only Q-branch transitions could be assigned. Nevertheless, it was possible to derive two vibration-rotation interaction constants, which agreed with those obtained from the ν_1 fundamental,[25] and three pure vibrational parameters that determine the structure of the $n\nu_1$ ladder. While some uncertainties remained, there was general agreement with the results of pulse probe measurements on the $2\nu_1 \leftarrow \nu_1$ transition that were reported simultaneously.[11]

Such studies of vibrational ladders have led to several interesting conclusions about the nature of excited vibrational states. In SiF_4, for example, the three components of the degenerate ν_4 stretching mode are strongly coupled, vibrational angular momentum is important, and its quantum number ℓ is appropriate to label the major energy level splittings. At the opposite extreme, the large UF_6 molecule has uncoupled vibrational motion with strong localization of the three individual components of ν_3, the splittings are best described with separate quantum numbers n_x, n_y, n_z for each of the

three orthogonal motions. SF_5 is an intermediate case and must be treated as a mixture of both types of motion. These cases are discussed in more detail in Ref. 37. The implications of these differences for the differing photochemical behavior of these molecules is just beginning to be explored.

5.3 Anharmonicity and Higher Vibrational Levels in General

For the interpretation of photochemical experiments, the higher levels of the pumped frequency (i.e., the $n\nu_1$ ladder for the spherical-top molecules we have been discussing) have attracted the most attention, as discussed in §5.1. The concept of anharmonicity, especially the effect of the constant X_{11}, here becomes crucial. For if a single-frequency laser pumps a molecular transition, resonance can be maintained for only the first few levels, after which the effect of X_{11} will detune the molecular absorption from the pump frequency. Absorption can still take place, of course, if this detuning is at least partially compensated for by anharmonic splitting of the higher levels (i.e., the effects of G_{11} and T_{11}), plus the influence of rotational structure, both of which can significantly broaden the higher level transitions.

Despite this inevitable attention to the $n\nu_1$ levels, it must be remembered that any molecule with n fundamentals has $n(n+1)/2$ anharmonicity constants X_{ij} governing the various possible overtone and combination levels. A full understanding of the excited-state structure requires that these be studied in addition to the $n\nu_1$ ladder. As one example, the state $\nu_2+\nu_6$ in SF_6 is at 991 cm^{-1}, just above ν_1 at 948 cm^{-1}, and it was proposed early in the study of SF_6 photochemistry that higher combinations of $\nu_2+\nu_6$ could help compensate for the anharmonicity detuning, through Fermi resonance between $n\nu_1$ and $(n-1)\nu_1+\nu_2+\nu_6$. [51] Other areas in which these considerations become important are in quantitatively accounting for the intensities of combination bands, understanding vibrational amplitudes in high-temperature electron diffraction experiments, and in the assignment and interpretation of the higher overtone and combination spectrum.

A reasonably detailed study of SF_6 overtone and combination bands has been made with a Fourier-transform instrument at a resolution of 0.05 cm^{-1}. [42,43] Twenty-nine bands were observed, of which 11 had sufficiently resolved rotational structure for a polynomial fit to be made, yielding such spectroscopic constants as the band origin and derived values of the rotational constant change $\Delta B = B' - B_0$ and the Coriolis constant ζ. An example is $2\nu_1+\nu_4$, shown in Fig. 7. Here the Coriolis constant (a measure of the vibrational angular momentum) was found to be $\zeta = 0.224$, about the value for ν_4 itself ($\zeta_4 = 0.210$), indicating that, as expected, the presence of the ν_1 excitation does not affect this aspect of vibration-rotation interaction.

For 17 other unresolved bands, accurate estimates of the band origin could be made from the frequency of a sharp Q-branch edge. Counting associated hot band transitions, some of which could be rotationally analyzed, a final data set of some 80 frequencies was available to determine the 21 anharmonicity constants of SF_6. Certain com-

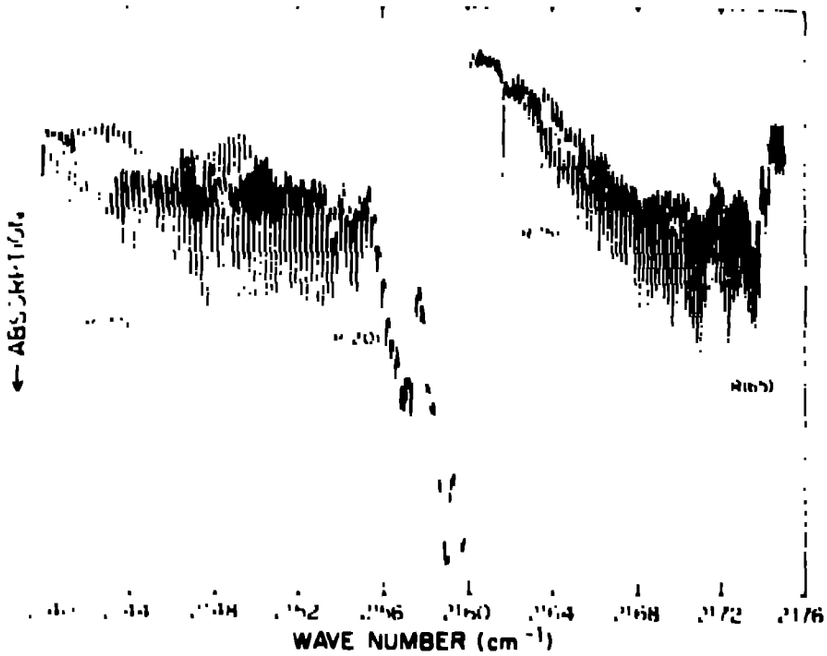

Fig. 7. One of the higher vibrational transitions in SF_6: $2\nu_3/\nu_4$, recorded at a resolution of 0.05 cm^{-1}. From reference 42.

plications peculiar to spherical tops affect this fitting procedure, and in some cases it was necessary to settle for "effective" constants X_{ij}', but in general the nature of the anharmonicity was clearly revealed.[41] All but one constant (X_{15}) could be determined, many with accuracies of 0.01 cm^{-1} or better. Almost all the constants are negative, and are less than 4 cm^{-1} in absolute magnitude. As a by product, accurate values of the fundamentals ν_5 and ν_6 were derived; ν_5 is Raman active only, and has never been resolved, while ν_6 is both infrared and Raman-inactive. Improvement on these data would require full Doppler limited or sub-Doppler spectra and analyses of each combination and overtone, a formidable task.

These constants can be used to construct a vibrational energy level diagram, Fig. 8.[44] Even with the extensive spectroscopic work on SF_6, it is necessary to make certain assumptions regarding the sub level and rotational structure of most of the levels, as indicated in the caption to Fig. 8. This still represents one of the more accurate depictions of extensive excited state structure that is available for any molecule. Excitation of the ν_3 ladder is indicated in the figure, together with some typical near resonant collisional pathways out of the ladder. It is to be noted that after only a few ν_3 quanta are absorbed, a near continuum of levels is accessible by leakage from the ladder, especially into higher states of the bending modes.

No other heavy spherical top has been treated as extensively as SF_6. Besides $^{34}SF_6$,[39] a start has been made on other combinations and overtones.[45] Other than $^{34}SF_6$[41] only ν_3/ν_4 has been investigated in any detail.[46] It is still possible to construct for these molecules approximately correct diagrams like Fig. 8, which can

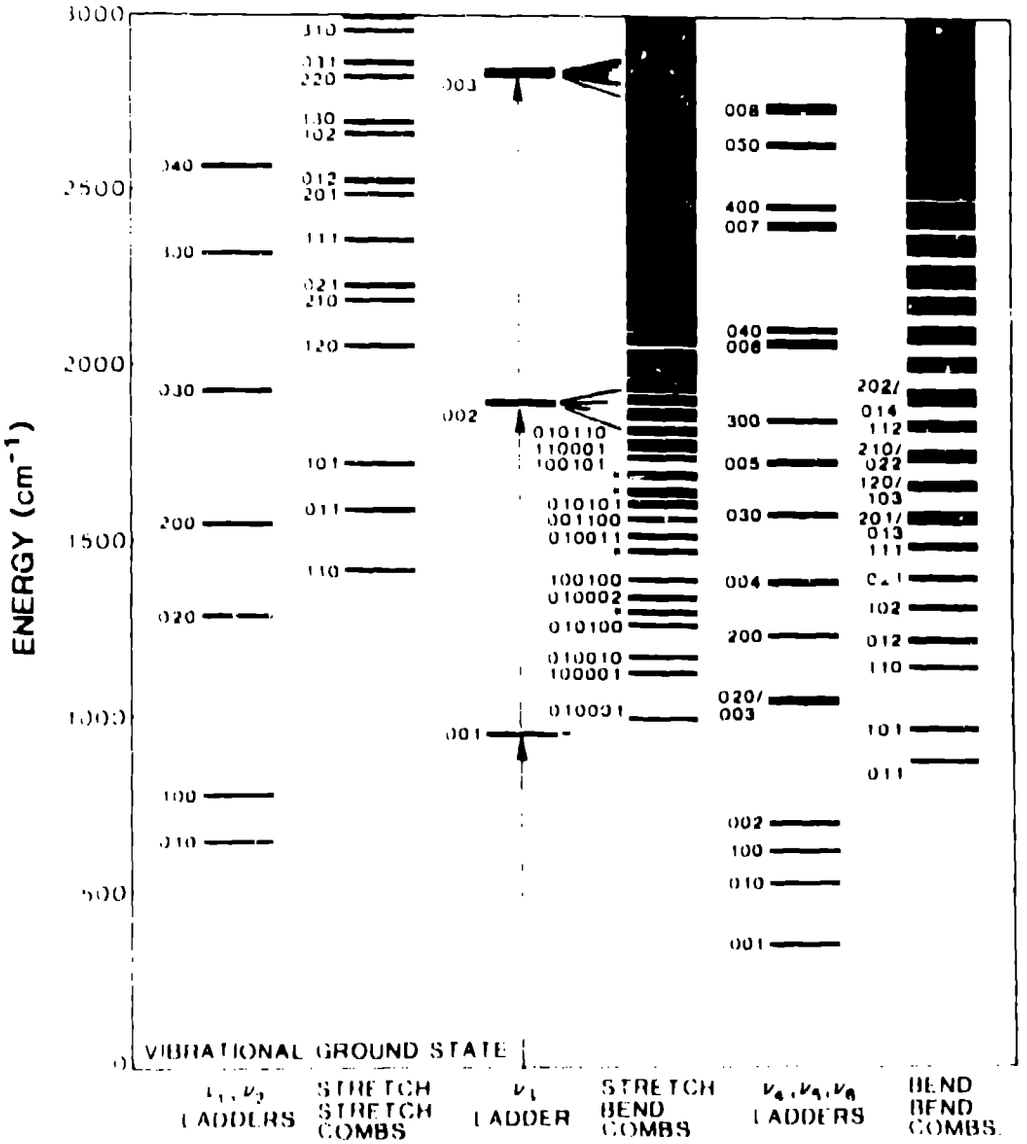

Fig. 8 Vibrational levels in SF_6 below 3000 cm^{-1}, illustrating intramolecular energy transfer in multiple photon excitation of the ν_3 ladder. The levels are labeled with the stretching quantum numbers $(n_1n_2n_3)$ in Cols. 1-3, the bending quantum numbers $(n_4n_5n_6)$ in Cols. 5 and 6, and all six in Col. 4. For vibrational states other than $3\nu_3$ and $3\nu_4$, anharmonic splittings of higher vibrational manifolds were arbitrarily assumed to be 1 cm^{-1}, and each sublevel was given a width of 12 cm^{-1} to indicate rotational broadening. From reference 44.

be used for discussing photochemical behavior.[73] For a given amount of ν_3 excitation, the accessibility of higher bending levels, compared with SF_6, is much less for SiF_4 and very much more for TiF_4. These characteristics will be discussed further in the next section.

6. VIBRATIONAL STATE DENSITIES AND PHOTOCHEMISTRY

An excellent critical discussion of laser-induced multiphoton excitation and dissociation of polyatomic molecules is given by Lyman *et al.*[7] They point out that the density of vibrational states is perhaps the most important molecular property in determining multiphoton-absorption characteristics: this state density defines the quasi continuum region, determines the unimolecular reaction rate in RRKM theory, and dominates the theory of intermode energy flow.

Calculation of the density of vibrational states for real molecules can be a lengthy process, and approximation methods are usually used. The best-known of these is the Whitten-Rabinovitch formula,[8] which gives the density of states $N(E_v)$ at vibrational energy E_v as a function of just four molecular parameters: the number of vibrational degrees of freedom, the arithmetic and geometric means of the fundamental vibrational frequencies, and a frequency dispersion parameter β which is also calculated from the frequencies. This formula is based on a "corresponding vibrational states" approximation, and includes an empirical correction parameter whose form was established by fitting to directly-calculated state densities for a variety of molecules.

We have undertaken an exact computation of the density of vibrational states for a series of spherical-top molecules, with the objects of (1) comparing these results with approximation methods, such as that of Whitten and Rabinovitch, and (2) determining the effect of anharmonicity. It should be emphasized that for spherical-top molecules, which have triply degenerate low-frequency bending fundamentals, the state density can be extremely high even with only moderate amounts of vibrational excitation. Hence the interest in anharmonicity, which can have a much greater effect on highly excited states than it does on levels with n ≤ 3 vibrational quanta, which are the ones usually encountered in spectroscopy.

Examples of these calculations for a few molecules at low vibrational energies are shown in Table 2. We note that the Whitten-Rabinovitch approximation is quite satisfactory at lower energies, but eventually anharmonicity begins to exert a significant effect. For SF_6, whose anharmonic constants are the best characterized among the heavy spherical tops, the increase in $N(E_v)$ due to anharmonicity is 6% at E_v = 5000 cm^{-1}, 18% at 10,000 cm^{-1} (these values from Table 2), and has reached 32% at 15,000 cm^{-1}. Other molecules would be expected to show similar increases at equivalent state densities. The relatively small increase for UF_6 at 5000 cm^{-1} is an artifact, due to the fact that the bending anharmonicity in this molecule is very poorly characterized,[9] and has probably been underestimated. For $Si(CH_3)_4$, the anharmonicity of the low frequency ASi-C-H bends at 60 to 80 cm^{-1} is completely unknown, so the anharmonic calculation can not be made.

Also of interest is the great contrast between the vibrational state densities of different species, amounting to a factor of 10 between CH_4 and $Si(CH_3)_4$ at E_v = 15,000 cm^{-1}. This is, of course, due to the presence of the very low frequency bends of $Si(CH_3)_4$ mentioned in the preceding paragraph, which have no counterpart in methane.

Table 2. Vibrational State Densities for Some Spherical Tops[a]

Molecule	$N(E_v)$, levels/cm^{-1}		
	E_v = 1000 cm^{-1}	5000 cm^{-1}	10000 cm^{-1}
CH_4	(0.002)	(0.07)	(0.93)
SiF_4	(0.12) 0.16	(79) 87	(3690) 5040
SF_6	(0.15) 0.17	(1090) 1160	(5.2×10^4) 6.1×10^5
UF_6	(17) 17	(2.4×10^6) 2.6×10^6	(3.6×10^7)
$Ni(CO)_4$	(185)	(2.6×10^8)	(1.0×10^{12})

[a] The figures in parentheses are the state densities in the harmonic approximation, from the Whitten-Rabinovitch formula; the other figures are the actual summed state densities with anharmonicity included

obviously the photochemical behavior of the molecules in Table 2 will be very different. A full discussion of these results, including plots like that of Fig. 8 for other species, and a detailed vibrational state density plot for all of these molecules for $E_v \leq 15{,}000$ cm^{-1}, is in preparation.[44]

REFERENCES

1. Bell, R. J., Introductory Fourier Transform Spectroscopy (Academic Press, New York, 1972).
2. Griffiths, P. R., and de Haseth, J. A., Fourier Transform Infrared Spectroscopy (John Wiley & Sons, New York, 1986).
3. Brault, J. W., J. Opt. Soc. Amer. 66, 1081 (1976).
4. Guelachvili, G., Appl. Opt. 17, 1322 (1978).
5. Kauppinen, J., Appl. Opt. 14, 1987 (1975); 18, 1788 (1979).
6. Palmer, B. A., "The Los Alamos Fourier Transform Spectrometer," Los Alamos National Laboratory Report LALP-85-16 (Aug. 1985).
7. Palmer, B. A., "Design and Characterization of the Los Alamos Fourier Transform Spectrometer," High Resolution Fourier Transform Spectroscopy, 1989 Technical Digest Series, Vol. 6 (Optical Society of America, Washington, D.C., 1989), pp. 52-55. This digest contains other papers of interest on Fourier transform spectroscopy.
8. McDowell, R. S., "Vibrational Spectroscopy Using Tunable Lasers," Vibrational Spectra and Structure (J. R. During, ed.) 10, 1-61 (Elsevier, Amsterdam, 1981).
9. McDowell, R. S., Proc. SPIE Int. Soc. Opt. Eng. 380, 96 (1984).
10. McDowell, R. S., Proc. Soc. Photo-Opt. Instrum. Eng. 113, 160 (1977).
11. McDowell, R. S., Galbraith, H. W., Krohn, B. J., Cantrell, C. D., and Hinkley, E. D., Opt. Commun. 17, 138 (1976).
12. McDowell, R. S., Galbraith, H. W., Cantrell, C. D., Peterson, T.

G., and Hinkley, E. D., J. Mol. Spectrosc. 68, 288 (1977).
13. McDowell, R. S., Galbraith, H. W., Cantrell, C. D., Nereson, N. G., Moulton, P. F., and Hinkley, E. D., Opt. Lett. 2, 97 (1978).
14. Brock, E. G., Krohn, B. J., McDowell, R. S., Patterson, C. W., and Smith, D. F., J. Mol. Spectrosc. 76, 301 (1979).
15. Loete, M., Clairon, A., Frichet, A., McDowell, R. S., Galbraith, H. W., Hilico, J.-C., Moret-Bailly, J., and Henry, L., Compt. Rend. Hebd. Seances Acad. Sci. (Paris), Sér. B 285, 175 (1977).
16. Kim, K. C., Person, W. B., Seitz, D., and Krohn, B. J., J. Mol. Spectrosc. 76, 322 (1979).
17. Bobin, B., Bordé, C. J., Bordé, J., and Bréant, C., J. Mol. Spectrosc. 121, 91 (1987).
18. Eshorick, P., and Owyoung, A., J. Mol. Spectrosc. 92, 162 (1982).
19. McDowell, R. S., Buchwald, M. I., Soren, M. S., Robiette, A. G., Dealey, C. M., and Kreiner, W. A., J. Mol. Spectrosc 112, 363 (1985).
20. Laux, L., Fov, B., Harradine, D., and Steinfeld, J. I., J. Chem. Phys. 80, 3499 (1984).
21. McDowell, R. S., Radziemski, L. J., Flicker, H., Galbraith, H. W., Kennedy, R. C., Nereson, N. G., Krohn, B. J., Aldridge, J. P., King, J. D., and Fox, K., J. Chem. Phys. 69, 1513 (1978).
22. Bobin, B., Valentin, A., and Henry, L., J. Mol. Spectrosc. 122, 229 (1987).
23. McDowell, R. S., Patterson, C. W., Nereson, N. G., Petersen, F. R., and Wells, J. S., Opt. Lett. 6, 422 (1981); errata, ibid. 647.
24. Patterson, C. W., McDowell, R. S., Nereson, N. G., Krohn, B. J., Wells, J. S., and Petersen, F. R., J. Mol. Spectrosc. 91, 416 (1982).
25. Aldridge, J. P., Brock, E. G., Filip, H., Flicker, H., Fox, K., Galbraith, H. W., Holland, R. F., Kim, K. C., Krohn, B. J., Magnuson, D. W., Maier, W. B., McDowell, R. S., Patterson, C. W., Person, W. B., Smith, D. F., and Werner, G. K., J. Chem. Phys. 81, 36 (1985).
26. Patterson, C. W., McDowell, R. S., Nereson, N. G., Begley, R. F., Galbraith, H. W., and Krohn, B. J., J. Mol. Spectrosc. 80, 71 (1980).
27. McDowell, R. S., Patterson, C. W., Jones, C. R., Buchwald, M. I., and Telle, J. M., Opt. Lett. 4, 274 (1979).
28. McDowell, R. S., Reisfeld, M. J., Galbraith, H. W., Krohn, B. J., Flicker, H., Kennedy, R. C., Aldridge, J. P. and Jereson, N. G., J. Mol. Spectrosc. 81, 440 (1980).
29. Patterson, C. W., McDowell, R. S., and Nereson, N. G., IEEE J. Quantum Electron. QE-16, 1164 (1980).
30. Hecht, K. T., J. Mol. Spectrosc. 5, 355 (1960).
31. Krohn, B. J., McDowell, R. S., Patterson, C. W., Nereson, N. G., Reisfeld, M. J., and Kim, K. C., J. Mol. Spectrosc. 132, 283 (1988).
32. Fildal, H., J. Chem. Phys. 67, 1287 (1977).
33. Ackerhalt, J. R., Flicker, H., Galbraith, H. W., Fing, J., and Person, W. B., J. Chem. Phys. 69, 1461 (1978).
34. Pine, A. S., and Robiette, A. G., J. Mol. Spectrosc. 80, 388 (1980).

35. Patterson, C. W., Krohn, B. J., and Pine, A. S., J. Mol. Spectrosc. 88, 133 (1981).
36. Patterson C. W., McDowell, R. S., Moulton, P. F., and Mooradian, A., Opt. Lett. 6, 93 (1981).
37. McDowell, R. S., Patterson, C. W., and Harter, W. G., Los Alamos Science 3(1), 38 (Winter/Spring 1982).
38. Patterson, C. W., and Pine, A. S., J. Mol. Spectrosc. 96, 404 (1982).
39. Harzer, R., Schweizer, G., and Selter, K., J. Mol. Spectrosc. 132, 310 (1988).
40. Fuss, W., Chem. Phys. Lett. 71, 77 (1980).
41. Hodgkinson, D. P., and Robiette, A. G., Chem. Phys. Lett. 82, 193 (1981).
42. McDowell, R. S., Krohn, B. J., Flicker, H., and Vasquez, M., Spectrochim. Acta 42A, 351 (1986).
43. McDowell, R. S., and Krohn, B. J., Spectrochim Acta 42A, 371 (1986).
44. McDowell, R. S., Krohn, B. J., and Lyman, J. L., to be published.
45. McDowell, R. S., Reisfeld, M. J., Patterson, C. W., Krohn, B. J., Vasquez, M. C., and Laguna, G. A., J. Chem. Phys. 77, 4337 (1982).
46. McDowell, R. S., Reisfeld, M. J., Nereson, N. G., Krohn, B. J., and Patterson, C. W., J. Mol. Spectrosc. 113, 243 (1985).
47. Lyman, J. L., Quigley, G. P., and Judd, O. P., in Multiple-Photon Excitation and Dissociation of Polyatomic Molecules (C. D. Cantrell, ed.) (Springer-Verlag, Berlin, 1986), pp. 9-94.
48. Whitten, G. Z., and Rabinovitch, B. S., J. Chem. Phys. 38, 2466 (1963).